Selective Tumor Cell Targeting Using Low-Affinity, Multivalent Interactions

Coby B. Carlson[†,‡], Patricia Mowery[‡], Robert M. Owen[†], Emily C. Dykhuizen[†], and Laura L. Kiessling[†,‡,§,]*

[†]Department of Chemistry, 1101 University Avenue, University of Wisconsin–Madison, Madison, Wisconsin 53706, [‡]Department of Biochemistry, 433 Babcock Drive, University of Wisconsin–Madison, Madison, Wisconsin 53706, and [§]University of Wisconsin Comprehensive Cancer Center, Madison, Wisconsin 53706

One hundred years have passed since Paul Ehrlich coined the term "magic bullet" to describe a chemotherapeutic that seeks out and kills disease-causing cells while leaving normal ones unaffected (1). This visionary concept remains an inspiration for many targeted drug strategies. Indeed, numerous anticancer drugs rely on the high-affinity monovalent interaction between a cell-binding agent (e.g., monoclonal antibody or fragment thereof) and a tumor-associated antigen to direct a cytotoxic moiety selectively to the tumor (2). Despite the potential advantages of this strategy, this mode of cell recognition is abiotic. One critical consequence of such non-natural recognition is that it often lacks the required selectivity. Thus, the toxin can also be delivered to normal cells with low levels of the target receptor.

In physiological systems, multiple low-affinity interactions are used to distinguish one cell type from another (3, 4). We have shown previously that a multivalent presentation can improve not only the affinity but also the specificity of ligand–receptor interactions (5, 6). On the basis of these results, we sought to compare the selectivity of a traditional cell-targeting approach to an alternative that mimics natural cell recognition processes.

Our multivalent targeting strategy exploits a preexisting immune response that poses a major barrier to xenotransplantation. The immunological differences between humans and most other mammals have prevented the transfer of tissue and organs across species (7). The galactosyl-(1−3)galactose (α-Gal) carbohydrate epitope is abundantly expressed on the surface of nearly all mammalian and bacterial cells (8). Humans, apes, and Old World monkeys, however, do not display α-Gal on their cell surfaces because they lack the functional glycosyltransferase that catalyzes the assembly of

ABSTRACT This report highlights the advantages of low-affinity, multivalent interactions to recognize one cell type over another. Our goal was to devise a strategy to mediate selective killing of tumor cells, which are often distinguished from normal cells by their higher levels of particular cell surface receptors. To test whether multivalent interactions could lead to highly specific cell targeting, we used a chemically synthesized small-molecule ligand composed of two distinct motifs: (1) an Arg-Gly-Asp (RGD) peptidomimetic that binds tightly ($K_d \approx 10^{-9}$ M) to $\alpha_v\beta_3$ integrins and (2) the galactosyl-α(1−3)galactose (α-Gal epitope), which is recognized by human anti-α-galactosyl antibodies (anti-Gal). Importantly, anti-Gal binding requires a multivalent presentation of carbohydrate residues; anti-Gal antibodies interact weakly with the monovalent oligosaccharide ($K_d \approx 10^{-5}$ M) but bind tightly ($K_d \approx 10^{-11}$ M) to multivalent displays of α-Gal epitopes. Such a display is generated when the bifunctional conjugate decorates a cell possessing a high level of $\alpha_v\beta_3$ integrin; the resulting cell surface, which presents many α-Gal epitopes, can recruit anti-Gal, thereby triggering complement-mediated lysis. Only those cells with high levels of the integrin receptor are killed. In contrast, doxorubicin tethered to the RGD-based ligand affords indiscriminate cell death. These results highlight the advantages of exploiting the type of the multivalent recognition processes used by physiological systems to discriminate between cells. The selectivity of this strategy is superior to traditional, abiotic, high-affinity targeting methods. Our results have implications for the treatment of cancer and other diseases characterized by the presence of deleterious cells.

*Corresponding author,
Kiessling@chem.wisc.edu.
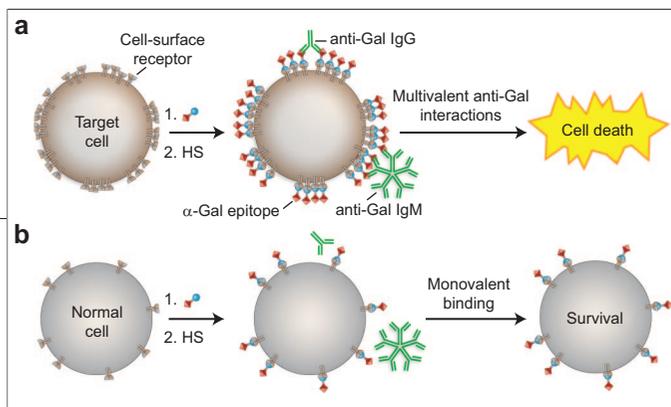
Figure 1. Graphical representation of cell-targeting strategy based on multivalent binding. A bifunctional conjugate ●–◆ (represented by the blue circles attached to red diamonds) binds with high affinity to a cell-surface receptor (*e.g.*, integrin) that is present in high concentration on a target cell. The blue circle represents an integrin ligand. The low-affinity α-Gal epitope (red diamond) recruits bivalent anti-Gal IgG (green) and decavalent anti-Gal IgM (green) when a noncovalent multivalent array is assembled on the cell surface. a) Cells displaying high levels of the target receptor recruit the antibody, which results in complement-mediated cell death. b) Cells with low levels of the target receptor are unaffected, because the monovalent anti-Gal interaction is weak.

this structure (*9*). Consequently, these species generate high concentrations of antibodies to this antigen. In humans, as much as 2% of the total IgG circulating in the bloodstream is anti-Gal (*10*), and the decavalent anti-Gal IgM isotype accounts for 3–8% of the total IgM (*10, 11*). These high antibody titers are maintained in humans throughout their lives, presumably in response to constant exposure to α-Gal found on bacteria within the normal intestinal flora (*12*).

Anti-Gal antibodies are potent activators of the classical complement pathway and are responsible for the hyperacute rejection of xenotransplanted organs (*13, 14*). Like many carbohydrate-binding proteins, anti-Gal antibodies interact only weakly with a single α-Gal epitope ($K_d \approx 10 \ \mu M$) but bind with higher functional affinity ($K_d \approx 10^{-11}$ M) to multivalent arrays of the saccharide (*15, 16*). Thus, the apparent binding affinity of anti-Gal is proportional to the valency of α-Gal epitopes presented. We envisioned, therefore, that anti-Gal antibodies could be recruited to selectively target unwanted cells that display high levels of α-Gal.

Bifunctional conjugates that bind to a cell-surface receptor and present α-Gal should render tumor cells susceptible to lysis. It has been shown that circulating antibodies can be redirected to a target cell using small molecules (*17–19*), and synthetic conjugates of α-Gal have been prepared (*20–23*). These studies, however, do not address the importance of multivalent binding, and the selectivity of such agents for cell targeting is unknown. Our objective was to test the utility and specificity of multivalent interactions for targeting cells (Figure 1). A synthetic bifunctional ligand, which uses noncovalent interactions to create a multivalent display on the cell surface, can recruit endogenous human anti-Gal antibodies to achieve highly selective cell killing.

RESULTS AND DISCUSSION

Design and Synthesis of Bifunctional Conjugates.

To test our hypothesis, we needed a model system with a cell-surface receptor that is up-regulated on target cells but produced only at low levels by normal cells. We selected the $\alpha_v\beta_3$ integrin. The integrins are a superfamily of heterodimeric proteins that mediate cell–cell attachment and cellular adhesion to the extracellular matrix (*24–26*); many integrins act through recognition of the RGD tripeptide motif (*27, 28*). The $\alpha_v\beta_3$ integrin is displayed in elevated levels on both invasive tumor cells and the endothelium of the tumor vasculature (*29–35*). Because $\alpha_v\beta_3$ is a potential therapeutic target in cancer research, a wide range of small-molecule ligands are known (*36–38*). Several of these compounds have been successfully modified for applications that include molecular imaging, gene therapy, radiotherapy, and targeted drug delivery (*38, 39*).

DeGrado and coworkers previously identified the nonpeptidic RGD mimetic **1** (Figure 2) as a ligand that binds potently and selectively to $\alpha_v\beta_3$ over related integrins (*40*). Guided by the structure of the extracellular segment of $\alpha_v\beta_3$ bound to a cyclic RGD peptide derivative (*41*), we devised compound **2** (Figure 2). This compound possesses a linker terminating in an amino group for subsequent modification. Like the parent ligand **1**, derivatives of **2** bind to $\alpha_v\beta_3$ with high affinity and selectivity (*42*). We used amine **2** to prepare three different bifunctional ligands. First, we treated compound **2** with fluorescein isothiocyanate to generate probe **3** (Figure 2), which provides a means to analyze the levels of $\alpha_v\beta_3$ on various cell lines. Second, we chemically modified doxorubicin (DOX) (*43*) so that it could be appended to compound **2** to yield the cytotoxic agent **4** (Figure 2). This conjugate should exert its deleterious effects subsequent to monovalent binding to the cell surface. Finally, we used conjugate **5**, which was generated *via* dimethyl squarate-mediated coupling (*44*) between compound **2** and the Galα(1–3)Galβ(1–4)Glc trisaccharide possessing an amine-bearing poly(ethylene glycol) linker (Figure 2) (*42*).

Evaluating Cell-Surface Receptor Levels. To investigate the ability of bifunctional conjugate **5** to selectively induce cytotoxicity, we required cells displaying varying amounts of $\alpha_v\beta_3$ integrin. Flow cytometry has been used previously to assess the concentration of both α_v and β_3 integrin subunits, as well as the heterodimer, on different cell lines (*34, 35, 45, 46*). Anti-

CARLSON *ET AL.*
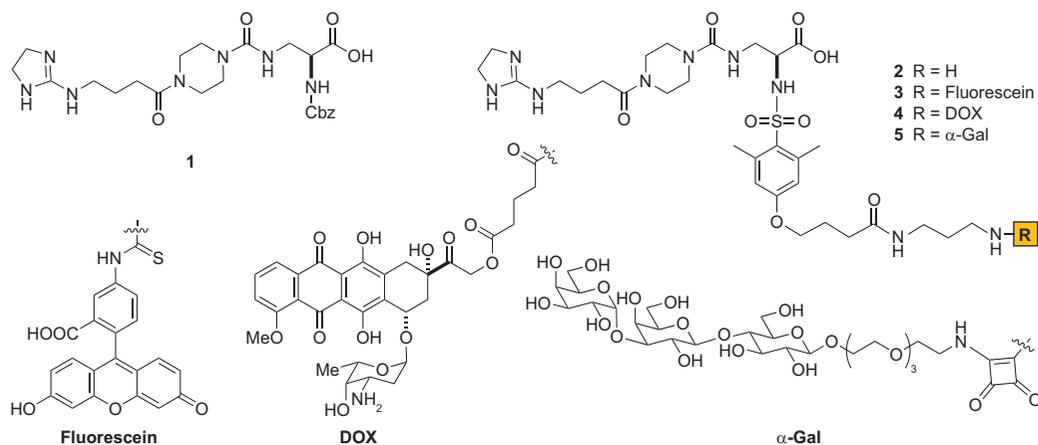
Figure 2. Chemical structures of small-molecule integrin ligands used in this study. The parent compound 1 is a peptido-mimetic that selectively binds the $\alpha_v\beta_3$ integrin. It inspired the design of 2, which bears a linker for conjugation to other moieties. Compound 2 can be functionalized to append a fluorophore (3), a cancer chemotherapeutic (4), or the α-Gal carbohydrate epitope (5).

bodies are typically used to measure integrin levels (*e.g.*, anti-human integrin monoclonal antibody followed by a secondary fluorescein-labeled antibody). The number of functionally active $\alpha_v\beta_3$ integrins on the cell surface, however, is the relevant parameter for our targeting strategy. Thus, we took a direct approach to detect those receptors accessible to the integrin ligand.

Using fluorescent integrin ligand 3, we determined the number of active $\alpha_v\beta_3$ integrins on the cell surface. We conducted titration experiments using nine different

human cancer cell lines, including 451Lu, 1205Lu, M21, MCF7, MDA-MB-231, Saos-2, SLK, WM115, and WM164. The modified integrin ligand bound with similar affinity to each cell type (average K_d value of 1.14 ± 1.05 nM; Figure 3, panel a, and Supporting Information). These results are consistent with previously reported binding data (*40*). We used a saturating concentration of probe 3 (10 nM) to measure the mean fluorescence intensity (MFI) for each cell line. In this way, we could compare MFI values (calibrated with fluorescent microspheres) to quantitate the levels of "targetable" $\alpha_v\beta_3$ integrin (Figure 3, panel b). M21 and WM115 cells displayed >100,000 receptors per cell, and we classified these levels as high. MCF7, MDA-MB-231, and Saos-2 cells had much lower levels of this integrin (<10,000 per cell). The amount of detectable cell-surface $\alpha_v\beta_3$ on the remaining cell lines (451Lu, 1205Lu, SLK, and WM164) was intermediate. Thus, with a series of cell lines possessing different amounts of the target receptor, we were poised to assess the importance of multivalent binding.
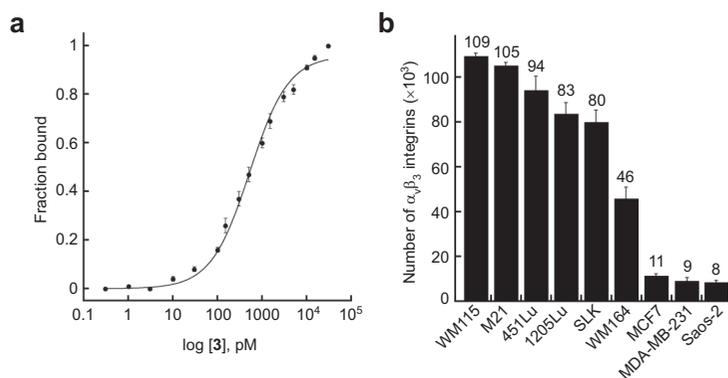
Figure 3. Analysis of $\alpha_v\beta_3$ integrin levels on target cell lines. a) A binding curve generated using flow cytometry for interaction of the fluorescein-labeled derivative 3 with WM115 cells. The apparent dissociation constant (K_d) for this interaction was 0.5 ± 0.04 nM. b) Histogram showing the number of cell-surface integrins measured using flow cytometry with a saturating concentration of derivative 3 (10 nM) and various cell lines.

a

b
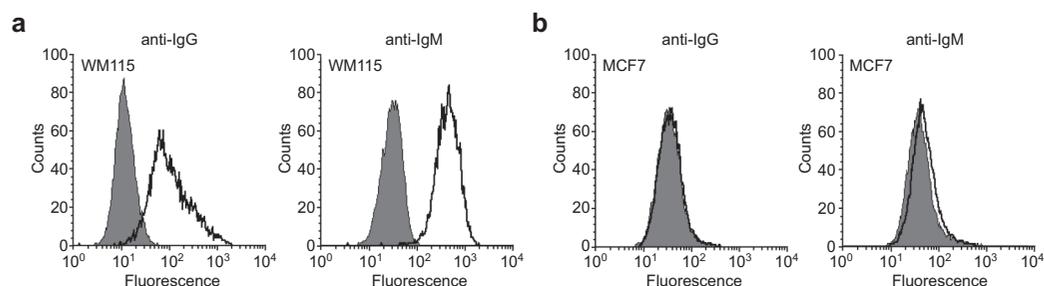
Figure 4. Recruitment of anti-Gal antibodies to the cell surface *via* binding of the bifunctional conjugate 5. Representa-tive flow cytometry plots illustrating the binding of anti-Gal IgG and IgM to a) WM115 cells (high levels of $\alpha_v\beta_3$) and b) MCF7 cells (low levels of $\alpha_v\beta_3$). The MFI was measured after cells were treated with 5, incubated with heat-inactivated HS, and labeled with fluorescein-conjugated goat anti-human IgG or IgM secondary antibodies. WM115 cells showed a positive log shift compared with untreated controls. No antibody binding was detected to MCF7 cells.

Cell and Antibody Binding of Bifunctional α-Gal Conjugate 5. For our synthetic conjugate to function as designed, it must simultaneously bind $\alpha_v\beta_3$ and anti-Gal antibodies. As mentioned above, we recently reported the utility of a series of α-Gal-conjugated RGD mimetics as cell-surface targeting agents and recruiters of anti-Gal antibodies (*38*). In the course of these studies, we devel-oped a fluorescence-based cell adhesion assay to test the binding of these ligands to integrins on cells. The measured IC$_{50}$ values for compound **1** and bifunctional conjugate **5** for $\alpha_v\beta_3$ were 8.1 $\pm$ 2 and 1.8 $\pm$ 0.2 nM, re-spectively (*42*). These data are consistent with previ-ously published data for the parent peptidomimetic (IC$_{50}$ value = 1.1 nM) (*40*).

When multiple copies of conjugate **5** bind to $\alpha_v\beta_3$ complexes on the cell surface, a multivalent display of α-Gal is assembled. To evaluate whether anti-Gal IgG and IgM antibodies can bind such a display, we ex-posed the WM115 and MCF7 cell lines to **5** and then to normal human serum (HS) (a source of anti-Gal). Washed cells were stained with fluorescein-labeled goat anti-human secondary antibodies and subse-quently analyzed by flow cytometry. The data indicate that WM115 cells, which display high levels of $\alpha_v\beta_3$, bind anti-Gal IgG and the higher valency IgM (Figure 4, panel a). In contrast, no anti-Gal antibody binding could be detected with MCF7 cells presenting low levels of $\alpha_v\beta_3$ (Figure 4, panel b). These results indicate that upon interaction of the conjugate with cell-surface integrin, anti-Gal can be recruited. Thus, both the anti-Gal-binding epitope and the integrin-binding moiety are ac-cessible to their protein targets (*42*). The finding that anti-Gal is recruited only to the cell displaying a high

level of $\alpha_v\beta_3$ integrin highlights the sensitiv-ity of anti-Gal binding to α-Gal epitope valency.

Cytotoxicity of the DOX Conjugate Does Not Depend on $\alpha_v\beta_3$ Levels. RGD-based peptides linked to the cytotoxic agent DOX can induce apoptosis in the tumor vascula-ture with enhanced effi-cacy and reduced cyto-toxicity (*47–49*).

Therefore, we envisioned that compound **4** could serve as an archetype of a traditional targeted chemothera-peutic. Using a standard tetrazolium salt-based method of assessing cell viability (*50*) with a variety of cell lines, we compared the cytotoxicity of **4** to that of free DOX. Upon treatment with compound **4**, we observed signifi-cant cytolysis (>50% dead) of each cell line tested (Figure 5, panel a); in contrast, cells were unaffected when exposed to the same concentration of free DOX (25 nM). Indeed, no significant cytotoxicity was ob-served with free DOX up to 0.5 μM (data not shown). These results emphasize a major problem associated with approaches that rely on monovalent interactions for cell killing: there is little discrimination between cells with low levels of the target receptor and those with high levels.

Conjugate 5 Is Only Cytotoxic to Cells with High $\alpha_v\beta_3$ Levels. To assess the cell-targeting selectivity of the α-Gal conjugate **5**, we employed a complement-dependent cytotoxicity assay. Briefly, cells were inter-nally labeled with a fluorescein diacetate esterase sub-strate, treated with compound **5**, and exposed to HS; the serum serves as the source of both anti-Gal antibod-ies and complement. If the bifunctional ligand can bind cell-surface $\alpha_v\beta_3$, recruit anti-Gal antibodies from HS, and activate the complement cascade, cytolysis would occur. Live cells were detected using a fluorescent plate reader. Untreated cells produce the maximum fluores-cence emission; a decrease in this signal corresponds to a decrease in the population of live cells, or cytotoxic-ity. We tested each of the cell lines and observed lysis (>60% dead) of five of the nine cell lines (Figure 5, panel b, red bars). Intriguingly, only those cells express-
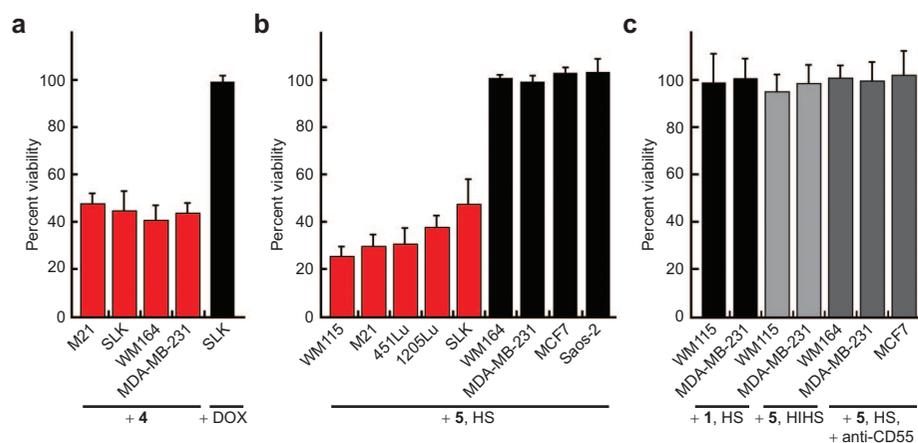
Figure 5. Bifunctional conjugate 5 mediates selective cell killing. a) The viability of four cell lines treated with compound 4 was evaluated using a standard tetrazolium-salt-based assay. Treatment with the DOX conjugate resulted in >50% cell death, irrespective of the levels of $\alpha_v\beta_3$ integrin (red). Unmodified DOX (25 nM) had no effect on the cells tested at this concentration (black). **b)** Data from all nine cell lines tested in the complement-dependent cytotoxicity assay. The cell lines that were lysed efficiently following treatment with bifunctional ligand 5 (10 nM) and HS are shown in red; those that were unaffected are depicted in black. **c)** Control experiments for the complement lysis assay are depicted. These include treatment with compound 1 (no α-Gal epitope) and HS (black), the α-Gal conjugate 5 and HIHS (light gray), and 5 with HS in the presence of an anti-CD55 function-blocking antibody (dark gray).

ing high levels of the target receptor were killed. For cell types with low levels of $\alpha_v\beta_3$, complement-mediated destruction was not observed (Figure 5, panel b).

The Cytotoxic Effects of Bifunctional Ligand 5 Depend on Complement-Mediated Lysis. We conducted several experiments to probe the mechanism of the observed cytotoxicity. First, we tested whether the cytotoxic response depends on the display of α-Gal moieties. When the parent compound 1 (which cannot recruit anti-Gal to the cell surface) was employed, no cell killing was observed (Figure 5, panel c). To determine whether the induced response was complement-mediated, we incubated cells with conjugate 5 and heat-inactivated HS (HIHS). This protocol should denature critical complement proteins but does not abolish anti-Gal antibody binding (10). Again, no lysis was detected (Figure 5, panel c, light gray bars). Finally, we sought to determine whether nonlysed cell lines were able to evade cellular destruction through the protective effects of one or more complement-regulating proteins (51). We used flow cytometry and monoclonal antibodies to known complement regulators (CD46, CD55, and CD59) to analyze three of the four cell lines that were not lysed (WM164, MDA-MB-231, and MCF7) and one that was destroyed (WM115). Only CD55, the receptor previously implicated in complement avoidance in

relation to anti-Gal (52), was present on the cell surface in significant amounts (see Supporting Information). When we repeated the experiment in the presence of an anti-CD55 antibody, which is known to block the protective function of CD55, no cytolysis was detected (Figure 5, panel c, dark gray bars). Together, these results indicate that the bifunctional ligand 5 is much more selective than traditional cell-targeting agents.

Enhancing Cell-Targeting Selectivity with Multivalency. The exquisite selectivity of α-Gal conjugate 5 contrasts dramatically with that observed for the DOX-linked compound 4. These differences can be visualized by comparing their relative cell-killing abilities (Figure 6, panel a). Our results with compound 4 are consistent with those of others in which the attachment of a "tumor-homing" agent to DOX results in selectivity for cells that display the target receptor over those that do not (47–49). Our data, however, underscore that this selectivity is limited. Thus, conjugates like 4 can kill cells with even low concentrations of targeted cell-surface receptor. Because it can be difficult to identify surface receptors unique to cancer cells, chemotherapeutic agents with such properties are expected to have deleterious side effects.

In contrast to 4, compound 5 is a highly discriminating cell-targeting agent. It can distinguish between cells
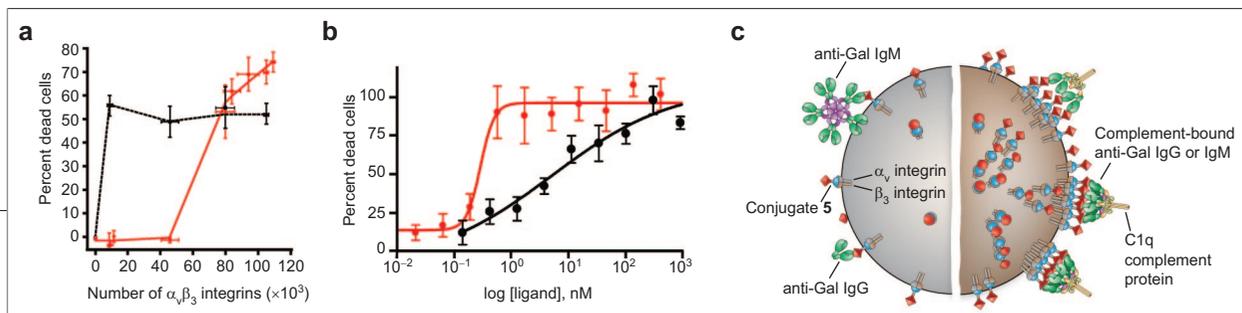
Figure 6. Features of cell recognition by multivalent interactions. a) The number of $\alpha_v\beta_3$ integrin receptors available for binding (data from Figure 3, panel b) is plotted against the percentage of dead cells (data from Figure 5, panel b). The dashed black curve describes the activity of the DOX conjugate 4. It kills cells displaying high and low levels of the target receptor. Conversely, cells with a low concentration of integrin receptor are unaffected by α-Gal-mediated cytotoxicity, as shown by the solid red curve. Bifunctional conjugate 5 results in selective lysis of cell lines with high levels of the target receptor. The cell death response is described by a curve with a much steeper slope and is similar to that displayed in panel b for compound 5. **b)** Dose response curves for compounds 4 (black) and 5 (red). Cell death by compound 5 displays a marked concentration dependence, an attribute indicative of a process involving cooperative multivalent interactions. The gradual dependence on concentration for the DOX conjugate 4 is typical of a process that involves monovalent interactions. **c)** A pictorial depiction of complement-mediated cell lysis through interaction with anti-Gal. This process involves several different types of multivalent interactions: anti-Gal binds avidly when it can interact with multiple α-Gal epitopes (as shown on the right), and complement is recruited more effectively when multiple copies of anti-Gal are bound.

with different levels of the target $\alpha_v\beta_3$ integrin receptor (Figure 6, panel a). One explanation for its remarkable selectivity is that cell killing is mediated through low-affinity, multivalent interactions. Because anti-Gal antibodies interact weakly with monovalent epitopes, any interaction with the α-Gal conjugate in solution will be transient. Similarly, anti-Gal is not recruited to cells displaying low levels of α-Gal residues. Only those cells with high levels of α-Gal residues on their surfaces can capture the bivalent (IgG) or decavalent (IgM) antibodies with sufficient avidity.

If cooperative multivalent interactions are critical for the activity of **5**, the concentration curves for cell killing by **5** should be steeper than those for **4**. Using WM115 cells, which possess high levels of $\alpha_v\beta_3$, we generated dose response curves for **4** and **5** (Figure 6, panel b). Compound **4** exhibits cytoxicity over a broad concentration range. In contrast, small changes in the concentration of bifunctional ligand **5** result in large changes in activity. These data provide further support that compound **4** functions *via* monovalent interactions but cell killing by compound **5** depends on multivalency.

Several steps in the cascade of events that culminate in complement-mediated cell lysis involve multivalency. When anti-Gal antibodies of the IgM class engage in multivalent interactions with the target cells, they expose a binding site for the multimeric C1q protein of the complement system. C1q binding initiates a cascade of protease activity, which results in the assembly of a membrane attack complex (MAC). It is this MAC that mediates lysis of the target cell. Thus, the complement system, which is composed of >30 proteins, also depends on multivalent interactions. Accordingly, our strategy exploits multivalent interactions for both cell recognition and cell killing by the immune system (Figure 6, panel c). Intriguingly, the data suggest that

there is a threshold response: only cells with sufficient levels of the target $\alpha_v\beta_3$ receptor are destroyed.

Exploiting Multivalency Using Low-Molecular-Weight Ligands. The strategy presented herein has advantages that go beyond its selectivity. Specifically, the mechanism by which the bifunctional ligands trigger cellular destruction does not rely on a non-natural toxin but rather on an endogenous immune response. Because humans are constantly exposed to the α-Gal antigen, a supply of anti-Gal in circulation is ensured. Moreover, unlike the situation with traditional toxins, the agent used for cell killing in our strategy (complement) is tightly controlled and therefore harmless to normal cells. Another major benefit of our strategy is that it employs low-molecular-weight compounds. Many tumor-targeting strategies rely on macromolecular agents, such as antibodies. Although the mode of action of our bifunctional ligands depends on multivalent recognition, the agents we describe are small-molecule ligands. As a consequence, they sidestep problems associated with macromolecular therapeutic agents.

A key feature of the design of our bifunctional conjugate is its modularity. The linkers, cell-surface targeting agent, and low-affinity epitope can be varied, thus affording the means to readily optimize the biological activity of the small molecules. Moreover, this design can be used to target more than one receptor on the cell surface. Another method to achieve selective cell targeting is to engage multiple types of up-regulated receptors. A highly selective cocktail of bifunctional ligands that bind and recruit complement to cancer cells, for example, would be extremely valuable. Finally, though we have presented our strategy in the context of cancer immunotherapy, we predict that this approach will have applications beyond tumor destruction.

Conclusion. As the mechanism of complement-mediated cell lysis indicates, physiological systems

CARLSON *ET AL.*

rely on low-affinity, multivalent interactions to distinguish between normal and unwanted target cells. An advantage of such processes is that highly specific recognition can be achieved. Our results indicate that the multivalent recognition mode that we employ can be exploited to selectively direct an endogenous immune response to destroy target cells. We envision that this general strategy and the principles underlying it will lead to new classes of therapeutic agents.

METHODS

Reagents. All chemicals used were purchased from Sigma-Aldrich unless otherwise noted. All cell culture reagents, including minimal essential medium alpha (αMEM), Dulbecco's modified eagle medium (DMEM), Roswell Park Memorial Institute-1640 medium (RPMI), fetal bovine serum (FBS), penicillin–streptomycin (pen–strep), L-glutamine, bovine insulin, and trypsin–EDTA, were purchased from Invitrogen. Accutase cell detachment solution was acquired from Innovative Cell Technologies, Inc. Tissue culture flasks for adherent cells were obtained from Sarstedt. 2′,7′-Bis-(2-carboxyethyl)-5-(and-6)-carboxy-fluorescein, acetoxymethyl ester (BCECF-AM) was purchased from Molecular Probes. Bovine serum albumin (BSA) was obtained from Research Organics. V-shaped 96-well plates were obtained from Nalge Nunc, International. Fibrinogen and vitronectin were from CalBiochem. Quantum FITC Premixed MESF Kit was from Bangs Laboratories, Inc. (Fishers, IN). Antibodies mouse anti-human integrin $\alpha_v\beta_3$ (clone LM609), mouse anti-human CD55, FITC-labeled rat anti-mouse IgG, and FITC-labeled goat anti-human IgG and IgM were purchased from Chemicon, International, Lab Vision Corporation, BD Biosciences, and Vector Laboratories, respectively.

Synthesis of Bifunctional Conjugates. Routes to the parent RGD peptidomimetic and its conjugation to the α-Gal trisaccharide epitope (compounds **1**, **2**, and **5**) have been published (42). The fluorescent derivative (compound **3**) was generated from the trifluoroacetate salt of amine **2** (1.4 mg, 0.0017 mmol, 1 equiv), which was dissolved in 50 mM borate buffer at pH 9 (100 μL). To this mixture, fluorescein isothiocyanate (0.7 mg, 1.1 equiv) in dimethylformamide (30 μL) was added. The reaction was stirred at RT for 4.5 h and then quenched with 0.2 M AcOH in H_2O (100 μL). The product was purified by HPLC on a Vydac C18 semi-prep column using a 30 min gradient of 0–50% (v/v) CH_3CN in H_2O containing 0.1% TFA (v/v) to yield conjugate **3** in 60% yield. Procedures for the synthesis of the DOX conjugate **4** are detailed in the Supporting Information.

Cell Lines. Human MDA-MB-231 and MCF7 breast carcinoma cells and WM115 melanoma cell lines were purchased from American Type Culture Collection. WM164, 451Lu, and 1205Lu human melanoma cells were obtained from Wistar Institute. M21 human melanoma cells (sorted for high levels of $\alpha_v\beta_3$) and Saos-2 osteosarcoma cells were provided by P.M. Sondel and S. Helfand (UW–Madison). SLK-1 Kaposi's sarcoma cell line was obtained from the National Institutes of Health (NIH) AIDS Research & Reference Reagent Program. All cells were grown either in αMEM, DMEM, or RPMI media with FBS (10%), pen–strep antibiotics (100 U), and glutamine (2 mM). MCF7 cells were grown as above with the addition of 0.01 mg mL^{-1} bovine insulin. Cells were detached from cell culture flasks with trypsin–EDTA for passage. For experiments, Accutase was used to minimize the effects of trypsin on $\alpha_v\beta_3$.

Anti-Gal Antibody Binding. Near confluent cells were harvested, washed, counted, and resuspended at a density of 4 × 10^5 cells mL^{-1} in integrin binding buffer [IB; 25 mM Tris-HCl, pH = 7.2, NaCl (150 mM), BSA (1.5% w/v), glucose (5 mM), MgCl$_2$ (1.5 mM), and MnCl$_2$ (1.5 mM)] for 60 min at 4 °C. Cells were

then diluted to 2 × 10^5 cells mL^{-1} and incubated with compound **5** (10 nM) on ice for 60 min. Cells were washed with IB and resuspended in a 20% solution of HIHS obtained from a healthy donor. After a 60 min incubation on ice, cells were washed again with IB and incubated again at 4 °C with FITC-conjugated goat anti-human IgG or IgM antibody (5 μg mL^{-1}) for 30 min. Finally, propidium iodide (PI, 5 μg mL^{-1}) was added to washed cells and immediately analyzed for fluorescence using a FACSCalibur flow cytometer (Becton Dickinson). Data were analyzed using CellQuest software (Becton Dickinson). An identical assay omitting the bifunctional conjugate assessed background fluorescence. The relative fluorescence is reported as the ratio above background. Experiments were repeated in triplicate.

Levels of Cell-Surface Integrin $\alpha_v\beta_3$. Near confluent cells were harvested with Accutase and activated in IB as described above. Cells were then diluted to 2 × 10^5 cells mL^{-1} and incubated with fluorescein-labeled compound **3** (10 nM) on ice for 60 min. Cells were washed twice before being analyzed for fluorescence by flow cytometry. The linearity of the instrument was first validated using the Quantum FITC Premixed MESF Kit, and a standard fluorescence curve was then generated. Taking the signal (MFI) measured from samples stained with **3**, the resulting value for molecules of equivalent soluble fluorescence (MESF) was determined. The MESF unit corresponds to the fluorescence intensity of a given number of pure fluorochrome molecules in solution and, in our case, is equal to the number of $\alpha_v\beta_3$ integrins on the cell surface. Experiments were repeated at least three different times for each cell line.

Complement-Dependent Cytotoxicity Assay. Confluent cultures of cells were detached with Accutase, washed, counted, and resuspended at 1.25 × 10^6 cells mL^{-1} in PBS. Cells were fluorescently labeled with BCECF-AM (0.2 μg mL^{-1}) for 30 min at 37 °C and then washed and diluted to 4 × 10^5 cells mL^{-1} for activation in binding buffer. After 60 min on ice, cells were further diluted to 2 × 10^5 cells mL^{-1}, and conjugate **5** (10 nM) was added. V-shaped 96-well microtiter plates were treated with 200 μL of "blocking buffer" [25 mM Na$_2$CO$_3$, pH = 9.6, BSA (1.5% w/v), and Tween-20 (0.5% w/v)] for 2 h at rt. The blocking solution was removed, and the wells washed three times with 200 μL of IB. Ten thousand cells per well were added to the rinsed wells in the presence of 20% normal HS and incubated for a minimum of 2 h at 37 °C. Following this period, cells were spun at 500 rpm for 10 min in an Allegra 6KR centrifuge (Beckman Coulter), and nonlysed cells were quantified as the fluorescent signal was read from the bottom on an EnVision 2100 plate reader (Perkin Elmer). For maximum cell lysis, the cationic detergent cetyltrimethylammonium bromide was added to the wells at a 2% (w/v) final concentration. The spontaneous release of fluorescence (background, BG) was determined without addition of conjugate **5**. Cytotoxicity is calculated by the following equation: [(sample − BG)(max − BG)$^{-1}$] × 100.

Cell Viability Assay for Determining Cytotoxicity of Conjugate 3. Confluent cultures of M21, WM164, MDA-MB-231, and Saos-2 cells were detached and resuspended in media at 100,000 cells mL^{-1} (M21 and WM164) or 250,000 cells mL^{-1} (MDA-MB-231 and Saos-2). One hundred microliters of these

cell suspensions were transferred to each well of a clear, flat-bottom 96-well microtiter plate (Corning) and incubated overnight. Wells were then treated with RGD–DOX conjugate **4** (25 nM) in DMEM for 18–24 h. All wells were then washed with fresh culture medium. Cytotoxicity was assessed using the Cell-Titer 96 AQueous non-radioactive cell proliferation assay kit from Promega. After addition of the 3-(4,5-dimethylthiazol-2-yl)-5-(3-carboxymethoxyphenyl)-2-(4-sulfophenyl)-2H-tetrazolium, inner salt solution, the plate was incubated for an additional 1–2 h. The absorbance at 490 nm was recorded using an ELx800 microplate reader from Bio-Tek Instruments, Inc. Maximum cell death was induced by adding a final concentration of 2% SDS (w/v) to 100 μL of the cell suspension. Untreated cells were considered to be "100% alive" in this assay. Cytotoxicity results are calculated by [sample − max][untreated − max]$^{-1}$ × 100 and are presented as percent viability. No significant cytotoxicity was observed with free DOX up to 0.5 μM.

Supporting Information Available: This material is free of charge *via* the Internet.

Competing Interests Statement: The authors declare that they have no competing financial interests.

REFERENCES

1. Winau, F., Westphal, O., and Winau, R. (2004) Paul Ehrlich—in search of the magic bullet, *Microbes Infect. 6*, 786–789.

2. Wu, A. M., and Senter, P. D. (2005) Arming antibodies: prospects and challenges for immunoconjugates, *Nat. Biotechnol. 23*, 1137–1146.

3. Mammen, M., Chio, S.-K., and Whitesides, G. M. (1998) Polyvalent interactions in biological systems: implications for design and use of multivalent ligands and inhibitors, *Angew. Chem., Int. Ed. 37*, 2755–2794.

4. Kiessling, L. L., Gestwicki, J. E., and Strong, L. E. (2000) Synthetic multivalent ligands in the exploration of cell-surface interactions, *Curr. Opin. Chem. Biol. 4*, 696–703.

5. Kiessling, L. L., Gestwicki, J. E., and Strong, L. E. (2006) Synthetic multivalent ligands as probes of signal transduction, *Angew. Chem., Int. Ed. 45*, 2348–2368.

6. Mortell, K. H., Weatherman, R. V., and Kiessling, L. L. (1996) Recognition specificity of neoglycopolymers prepared by ring-opening metathesis polymerization, *J. Am. Chem. Soc. 118*, 2297–2298.

7. Galili, U. (2001) The α-gal epitope (Galα1−3Galβ1−4GlcNAc-R) in xenotransplantation, *Biochimie 83*, 557–563.

8. Galili, U., Clark, M. R., Shohet, S. B., Buehler, J., and Macher, B. A. (1987) Evolutionary relationship between the natural anti-Gal antibody and the Galα(1→3)Gal epitope in primates, *Proc. Natl. Acad. Sci. U.S.A. 84*, 1369–1373.

9. Galili, U., Shohet, S. B., Kobrin, E., Stults, C. L. M., and Macher, B. A. (1988) Man, apes, and Old World monkeys differ from other mammals in the expression of α-galactosyl epitopes on nucleated cells, *J. Biol. Chem. 263*, 17755–17762.

10. Galili, U., Rachmilewitz, E. A., Peleg, A., and Flechner, I. (1984) A unique natural human IgG antibody with anti-α-galactosyl specificity, *J. Exp. Med. 160*, 1519–1531.

11. Parker, W., Bruno, D., Holzknecht, Z. E., and Platt, J. L. (1994) Characterization and affinity isolation of xenoreactive human natural antibodies, *J. Immunol. 153*, 3791–3803.

12. Galili, U., Mandrell, R. E., Hamadeh, R. M., Shohet, S. B., and Griffiss, J. M. (1988) Interaction between human natural anti-α-galactosyl IgG and bacteria of the human flora, *Infect. Immun. 56*, 1730–1737.

13. Sandrin, M. S., Vaughan, H. A., Dabkowski, P. L., and McKenzie, I. F. C. (1993) Anti-pig IgM antibodies in human serum react predominantly with Gal(α1−3)Gal epitopes, *Proc. Natl. Acad. Sci. U.S.A. 90*, 11391–11395.

14. Mollnes, T. E., and Fiane, A. E. (2003) Perspectives on complement in xenotransplantation, *Mol. Immunol. 40*, 135–143.

15. Wieslander, J., Maansson, O., Kallin, E., Gabrielli, A., Nowack, H., and Timpl, R. (1990) Specificity of human antibodies against Galα(1−3)Gal carbohydrate epitope and distinction from natural antibodies reacting with Galα(1−2)Gal or Galα(1−4)Gal, *Glycoconjugate J. 7*, 85–100.

16. Wang, J.-Q., Chen, X., Zhang, W., Zacharek, S., Chen, Y., and Wang, P. G. (1999) Enhanced inhibition of human anti-Gal antibody binding to mammalian cells by synthetic α-Gal epitope polymers, *J. Am. Chem. Soc. 121*, 8174–8181.

17. Shokat, K. M., and Schultz, P. G. (1991) Redirecting the immune response: ligand-mediated immunogenicity, *J. Am. Chem. Soc. 113*, 1861–1862.

18. Bertozzi, C. R., and Bednarski, M. D. (1992) A receptor-mediated immune response using synthetic glycoconjugates, *J. Am. Chem. Soc. 114*, 5543–5546.

19. Lussow, A. R., Buelow, R., Fanget, L., Peretto, S., Gao, L., and Pouletty, P. (1996) Redirecting circulating antibodies *via* ligand–hapten conjugates eliminates target cells *in vivo*, *J. Immunother. 19*, 257–265.

20. Li, J., Zacharek, S., Chen, X., Wang, J., Zhang, W., Janczuk, A., and Wang, P. G. (1999) Bacteria targeted by human natural antibodies using α-Gal conjugated receptor-specific glycopolymers, *Bioorg. Med. Chem. 7*, 1549–1558.

21. Chen, Y., Zhang, W., Chen, X., Wang, J., and Wang, P. G. (2001) αGal-conjugated anti-rhinovirus agents: chemo-enzymatic syntheses and testing of anti-Gal binding, *J. Chem. Soc., Perkin Trans. 1*, 1716–1722.

22. Holle, L., Song, W., Hicks, L., Holle, E., Holmes, L., Wei, Y. Z., Li, J. H., Wagner, T., and Yu, X. Z. (2004) *In vitro* targeted killing of human endothelial cells by coincubation of human serum and NGR peptide conjugated human albumin protein bearing α(1-3) galactose epitopes, *Oncol. Rep. 11*, 613–616.

23. Naicker, K. P., Li, H., Heredia, A., Song, H., and Wang, L.-X. (2004) Design and synthesis of αGal-conjugated peptide T20 as novel antiviral agent for HIV-immunotargeting, *Org. Biomol. Chem. 2*, 660–664.

24. Hynes, R. O. (1992) Integrins—versatility, modulation, and signaling in cell-adhesion, *Cell 69*, 11–25.

25. Clark, E. A., and Brugge, J. S. (1995) Integrins and signal-transduction pathways—the road taken, *Science 268*, 233–239.

26. Giancotti, F. G., and Ruoslahti, E. (1999) Transduction–integrin signaling, *Science 285*, 1028–1032.

27. Ruoslahti, E., and Pierschbacher, M. D. (1987) New perspectives in cell-adhesion—RGD and integrins, *Science 238*, 491–497.

28. Plow, E. F., Haas, T. A., Zhang, L., Loftus, J., and Smith, J. W. (2000) Ligand binding to integrins, *J. Biol. Chem. 275*, 21785–21788.

29. Brooks, P. C., Montgomery, A. M. P., Rosenfeld, M., Reisfeld, R. A., Hu, T. H., Klier, G., and Cheresh, D. A. (1994) Integrin $\alpha_V\beta_3$ antagonists promote tumor-regression by inducing apoptosis of angiogenic blood-vessels, *Cell 79*, 1157–1164.

30. Hynes, R. O. (2002) A reevaluation of integrins as regulators of angiogenesis, *Nat. Med. 8*, 918–921.

31. Friedlander, M., Brooks, P. C., Shaffer, R. W., Kincaid, C. M., Varner, J. A., and Cheresh, D. A. (1995) Definition of two angiogenic pathways by distinct α_v integrins, *Science 270*, 1500–1502.

32. Pasqualini, R., Koivunen, E., and Ruoslahti, E. (1997) αv integrins as receptors for tumor targeting by circulating ligands, *Nat. Biotechnol. 15*, 542–546.

33. Arap, W., Pasqualini, R., and Ruoslahti, E. (1998) Cancer treatment by targeted drug delivery to tumor vasculature in a mouse model, *Science 279*, 377–380.

34. Wong, N. C., Mueller, B. M., Barbas, C. F., Ruminski, P., Quaranta, V., Lin, E. C., and Smith, J. W. (1998) α_v integrins mediate adhesion and migration of breast carcinoma cell lines, *Clin. Exp. Metastasis 16*, 50–61.

35. Allman, R., Cowburn, P., and Mason, M. (2000) *In vitro* and *in vivo* effects of a cyclic peptide with affinity for the $\alpha_v\beta_3$ integrin in human melanoma cells, *Eur. J. Cancer 36*, 410–422.

36. Miller, W. H., Keenan, R. M., Willette, R. N., and Lark, M. W. (2000) Identification and *in vivo* efficacy of small-molecule antagonists of integrin $\alpha_v\beta_3$ (the vitronectin receptor), *Drug Discovery Today 5*, 397–408.

37. Cacciari, B., and Spalluto, G. (2005) Nonpeptidic $\alpha_v\beta_3$ antagonists: recent developments, *Curr. Med. Chem. 12*, 51–70.

38. Meyer, A., Auemheimer, J., Modlinger, A., and Kessler, H. (2006) Targeting RGD recognizing integrins: drug development, biomaterial research, tumor imaging and targeting, *Curr. Pharm. Des. 12*, 2723–2747.

39. Temming, K., Schiffelers, R. M., Molema, G., and Kok, R. J. (2005) RGD-based strategies for selective delivery of therapeutics and imaging agents to the tumour vasculature, *Drug Resist. Updates 8*, 381–402.

40. Corbett, J. W., Graciani, N. R., Mousa, S. A., and DeGrado, W. F. (1997) Solid-phase synthesis of a selective $\alpha_v\beta_3$ integrin antagonist library, *Bioorg. Med. Chem. Lett. 7*, 1371–1376.

41. Xiong, J.-P., Stehle, T., Zhang, R., Joachimiak, A., Frech, M., Goodman, S. L., and Arnaout, M. A. (2002) Crystal structure of the extracellular segment of integrin $\alpha_v\beta_3$ in complex with an Arg-Gly-Asp ligand, *Science 296*, 151–155.

42. Owen, R. M., Carlson, C. B., Xu, J., Mowery, P., Fasella, E., and Kiessling, L. L. (2006) Bifunctional ligands that target cells displaying the $\alpha v\beta 3$ integrin, *ChemBioChem 8*, 68–82.

43. Nagy, A., Schally, A. V., Armatis, P., Szepeshazi, K., Halmos, G., Kovacs, M., Zarandi, M., Groot, K., Miyazaki, M., Jungwirth, A., and Horvath, J. (1996) Cytotoxic analogs of luteinizing hormone-releasing hormone containing doxorubicin or 2-pyrrolinodoxorubicin, a derivative 500–1000 times more potent, *Proc. Natl. Acad. Sci. U.S.A. 93*, 7269–7273.

44. Tietze, L. F., Arlt, M., Beller, M., Gluesenkamp, K. H., Jaehde, E., and Rajewsky, M. F. (1991) Squaric acid diethyl ester: a new coupling reagent for the formation of drug biopolymer conjugates. Synthesis of squaric acid ester amides and diamides, *Chem. Ber. 124*, 1215–1221.

45. Samaniego, F., Young, D., Grimes, C., Prospero, V., Christofidou-Solomidou, M., DeLisser, H. M., Prakash, O., Sahin, A. A., and Wang, S. Z. (2002) Vascular endothelial growth factor and Kaposi's sarcoma cells in human skin grafts, *Cell Growth Differ. 13*, 387–395.

46. Dickerson, E. B., Akhtar, N., Steinberg, H., Wang, Z. Y., Lindstrom, M. J., Padilla, M. L., Auerbach, R., and Helfand, S. C. (2004) Enhancement of the antiangiogenic activity of interleukin-12 by peptide targeted delivery of the cytokine to $\alpha_v\beta_3$ integrin, *Mol. Cancer Res. 2*, 663–673.

47. Arap, W., Pasqualini, R., and Ruoslahti, E. (1998) Cancer treatment by targeted drug delivery to tumor vasculature in a mouse model, *Science 279*, 377–380.

48. de Groot, F. M. H., Broxterman, H. J., Adams, H., van Vliet, A., Tesser, G. I., Elderkamp, Y. W., Schraa, A. J., Kok, R. J., Molema, G., Pinedo, H. M., and Scheeren, H. W. (2002) Design, synthesis, and biological evaluation of a dual tumor-specific motive containing integrin-targeted plasmin-cleavable doxorubicin prodrug, *Mol. Cancer Ther. 1*, 901–911.

49. Burkhart, D. J., Kalet, B. T., Coleman, M. P., Post, G. C., and Koch, T. H. (2004) Doxorubicin-formaldehyde conjugates targeting $\alpha_v\beta_3$ integrin, *Mol. Cancer Ther. 3*, 1593–1604.

50. Mosmann, T. (1983) Rapid colorimetric assay for cellular growth and survival: application to proliferation and cytotoxicity assays, *J. Immunol. Methods 65*, 55–63.

51. Morgan, B. P., and Meri, S. (1994) Membrane-proteins that protect against complement lysis, *Springer Semin. Immunopathol. 15*, 369–396.

52. Jager, U., Takeuchi, Y., and Porter, C. D. (1999) Induction of complement attack on human cells by Gal(alpha1,3)Gal xenoantigen expression as a gene therapy approach to cancer, *Gene Ther. 6*, 1073–1083.